# TUDaBo SAR-RDSAR for ESA Altimetry Virtual Lab Version 1.7

## Altimetry Coastal and Open Ocean Performance

## Product Validation Report (PVR)

## HYDROCOASTAL CCN1 D1.2 & D1.5

Project reference: TUDaBo_SAR-RDSAR PVR
Issue: 1.1

15th August 2023

**ESA Reference number: EOEP-SEOM-EOPS-PVR-1-1**

This page has been intentionally left blank

# Change Record

| Date | Issue | Section | Page | Comment |
|---|---|---|---|---|
| 20/03/2022 | 1.1 | | | First version |
| | 1.2 | | | 1st revision |
| 07/07/2022 | 1.3 | | | 2nd revision |
| 17/08/2023 | 1.4 | | | 3rd Revision |
| | | | | |
| | | | | |

# Control Document

| Process | Name | Date |
|---|---|---|
| Written by: | L. Fenoglio-Marc | 18/08/2023 |
| Checked by | C.Buchhaupt | |
| Approved by: | | |

| | Signature | Date |
|---|---|---|
| For Uni Bonn | | |
| For ESA: J. Benveniste | 'Date: 2023.09.28 10:56:20 +02'00 | Digitally signed by Jérôme Benveniste |

# Table of Contents

**Table of Contents** **4**

**1 Introduction** **5**
*1.1 Purpose and scope* *5*

**2 Analysis** **7**
*2.1 Cryosat-2* *7*
*2.2 Sentinel-3* *11*

**3 Validation** **12**
*3.1 Region and input data* *12*
*3.2 Post-Processing* *13*

**4 References** **23**

# 1 Introduction

## 1.1 Purpose and scope

This Product Validation Report (D1.2 in Table 1) is a merged document including CCN1 D1.2 and D1.5 (see planned deliveries in Table 1) and it is labelled CCN1 D1.2 & D1.5.

Two regions of interest (ROI) are considered: the North Eastern Atlantic ($ROI_1$-NEA) and in the Pacific Ocean ($ROI_2$-PB). The first ROI, which presents a large variability of wave heights and wave periods, is selected to study the effect of the vertical velocity on the geophysical parameters derived from the retracking.
The second ROI, which presents high geoid slopes particularly in the Marianna Trench, is of interest to study the effect of using the RMC processing instead of the SAR processing.

The goals of the proposal have been slightly revised. We substitute LRMC-F with LRMC processed by Back Projection Algorithm (BPA) (L1B.Focus_DDA=1) and use only one burst (L1B.Focus_Nb=1). We did found that results of "LRMC-F focused with four bursts" and "LRMC with Back Projection Algorithm (BPA) and one burst" are similar. The second processing is 10 times faster than the first.

For the first Region of interest in the North-East Atlantic ($ROI_1$-NEA), we deliver the Test Data Set 1 (D1.1) and Test Data Set 2 (D1.4) for Cryosat-2 and Sentinel-3 in the German Bight and Western Baltic Sea, sub-region ($ROI_1$-NEA/GBWB). The ATBD CCN1 **D1.3** of Version 1.7 is available. The 4 bursts are substituted by 1 burst.

The executable for Version 1.6 (**D1.6**), including the VMWP, is running in Earth Console. Version 1.7 (**D1.7**) will be soon available. Processor version 1.7 is a software program with routines in matlab and in C. The advantage of the C routines is to speed up the computation. While TUDaBo Processor version 1.6 was a "Matlab-only" version, the main novelty in version 1.7 is the mixed C and Matlab coding to speed computation. Two options exist from the L1A to L1B Processing: the unfocused DDA Algorithm (UF) (Raney, 1992) and a Back-Projection Algorithm (BPA) (Egido and Smith, 2017). The BPA is expected to be more correct, as it implicitly considers the range-walk and other processing also used in the focused (Fully focused) SAR processing. The BPA is slower when using unfocused DDA. The choice of 0/1 for the parameter L1B.Focus_DDA selects state of the art or BPA respectively.

The final processor is finally implemented on the TUDaBo ESA's Earth Console service with:

1. RDSAR
2. unfocused SAR (state of the art/BPA)
3. LRMC-SAR (state of the art/BPA)

The three retrackers used in this study, called SINC2, SINCS, SINCS-OV, are numerical retrackers. They use a numerical model and compute numerically the double convolution of the radar equation using the

real radar PTR. They can also be called semi-numerical, because, while the 2D inverse transform is computed numerically, 2D Fourier transform is computed analytically.
The relevant point is that they use the time evolving ptr. Using in-flight measured ptr is key to getting accurate values for ssh and swh which goes into ssb. The use of a constant ptr in SAR retrackers has been found to be the main point for the bias and drifts (OSTST 2022). On the opposite, the more standard Brown model is an analytical model using mathematical expression with approximations, and the Ice2 retracker is a non-parametric retracker which is not numerical, as the three indicated above, and which does not use a time evolving in-flight measured ptr.

Table 1.

| | |
|---|---|
| D1.1 | Test Data Set 1: L2, RDSAR, SAR and LRMC-SAR |
| D1.2 | Product Validation Report of D1.1 |
| D1.3 | ATBD for TuDaBo processor including VMWP |
| D1.4 | Test Data Set 2: L2,unfocused SAR and LRMC—F SAR with VMWP |
| D1.5 | Product Validation Report of D1.4 |
| D1.6 | SW executables for TuDaBo processor including VMWP (implemented on G-POD) |

Table 2 recalls the processing parameters.

**Table 2.** Options in the TUDaBo Processing for version 1.6/1.7 (see also Table 1 in CCN proposal)

| | | | |
|---|---|---|---|
| **Mission** | CS2, S3A, S3B | **Reference Ellipsoid** | WGS84, TOPEX, GRS80 |
| **Processing Mode** | RDSAR, SAR, LRMC-SAR | **Local Surface Approximation**<br>**L1B.REF_SURF** | Sphere, Ellipsoid, Slopes<br>**Geoid** |
| **Pulse Distribution** | Exponential<br>Zero Skewness Weibull<br>L1B.Pulse_Skew = 0/1 | **Use Hamming**<br>L1B.Win_Name_ts = hamming/rect<br>L1B.Win_Name_tf = hamming/rect | Yes, No |
| **L1B Sampling Frequency** | 20Hz, 40Hz, 80Hz<br>L1B.Sample_Freq = 20,40,80 | **Zero Padding** | Yes (always) |
| **Retracked Surface** | Water, Ocean, All, None<br>L2.RET_SURF = All | **Retracker RDSAR** | BMLE3, SINC2, TALES<br>NONE |
| **Retracker SAR** | SINCS, SINCS-OV, NONE | **Retracker**<br>**LRMC-SAR** | SINCS, **SINCS-OV**<br>NONE |
| **Dump Waveforms** | Yes, No | **Dump Stacks** | Yes, No |
| **Processing Algorithm** | L1B.Focus_DDA=0(UF), 1(BPA) | | |

# 2 Analysis

## 2.1 Cryosat-2

First we consider CryoSat-2 runs. Table 2 gives the list of the configuration files used for the runs. The first four correspond to Task1 and do not account for the Vertical Motion of Wave Particles (VMWP), the other four correspond to Task 2, dealing with the VMWP (Buchhaupt at al. 2017, 2019; Buchhaupt 2019). Bold configs in Table 2 involve unfocused SAR DDA processing, the other use the the Back Projection Algorithm. For each parameter, different choices have been considered, see Table 1. We adopt the option "geoid" and zero padding (see "bold" in config below in this section). Three retrackers are used: in RDSAR processing we have the retracker SINC2, in SAR and LRMC-SAR processing we have the two retrackers SINCS and SINCS_OV (see ATBD session 4.2).
For the distribution for the pulses in the stack two options are available: the exponential distribution and the zero-skewness Weibull distribution (see ATBD session 3.1.1.9).
Figs 1, 2, 3 show some results of the tests. Both waveform and RIP are smoother in LRMC-SAR than in SAR Processing with retracker SINCS (Fig. 1). The stack is shown in Fig. 2. Use of hamming windows gives standard deviation differences of 9 cm in uncorrected range and 35 cm in significant wave heights and 0.06 dB in backscatter coefficient. The biases are small.

The configs of the runs are listed in Table 3 and available via ftp as the output files for year 2018 .

Table 3. Configs for CS2 and S3A in Version 1.7. UF (bold) stands for unfocused SAR (or DDA), F stands for back projection

| Name of file | Processing Type | Pulse Distr. | Retracker | L1B.Focus_DDA |
|---|---|---|---|---|
| **config_UF1_STD.txt** | **UF1** | **STD** | **SINC2, SINCS, SINCS** | **0** |
| **config_UF1_ZSK.txt** | **UF1** | **ZSK** | **SINC2, SINCS, SINCS** | **0** |
| config_F1_STD.txt | F1 | STD | SINC2, SINCS, SINCS | 1 |
| config_F1_ZSK.txt | F1 | ZSK | SINC2, SINCS, SINCS | 1 |
| | | | | |
| **config_UF1_STD_OV.txt** | **UF1** | **STD** | **SINC2, SINCS_OV, SINCS_OV** | **0** |
| **config_UF1_ZSK_OV.txt** | **UF1** | **ZSK** | **SINC2, SINCS_OV, SINCS_OV** | **0** |
| config_F1_STD_OV.txt | F1 | STD | SINC2, SINCS_OV, SINCS_OV | 1 |
| config_F1_ZSK_OV.txt | F1 | ZSK | SINC2, SINCS_OV, SINCS_OV | 1 |

*UF1 data and UF1+F1 configs made available in sftp (21.03.2022 LF) are as following:
CS2 from version 1.7 inhouse, UF1 data and UF1+F1 configs, 21.03.2022 LF
S3A from version 1.6 GPOD, UF1 data and UF1 configs, 21.03.2022 LF
all UF1 data & UF1+F1 configs are in /shares/nis/tudabo/nasproj/CCN1/deliverableCCN_2ESA

CS2 from version 1.7 inhouse, F1 data and F1 configs as above, 15.04.2022 LF in /shares/nis/tudabo/nasproj/CCN1/deliverables

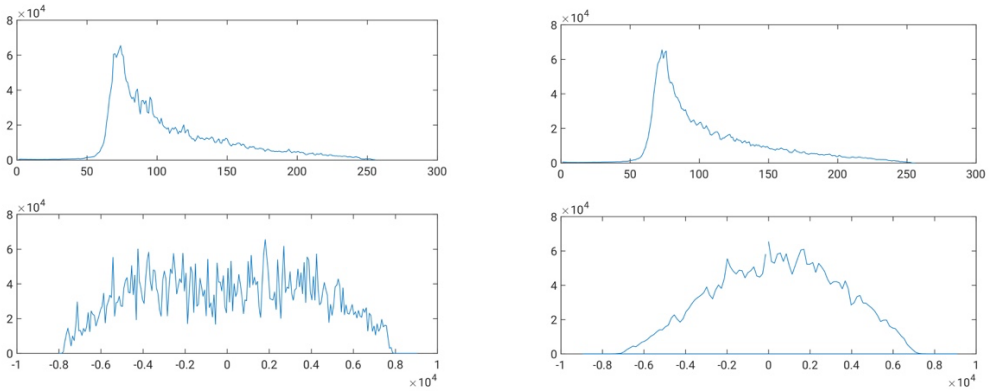

Fig.1 CS2. Waveform and RIP of SAR (left) and LRMC-SAR (right).

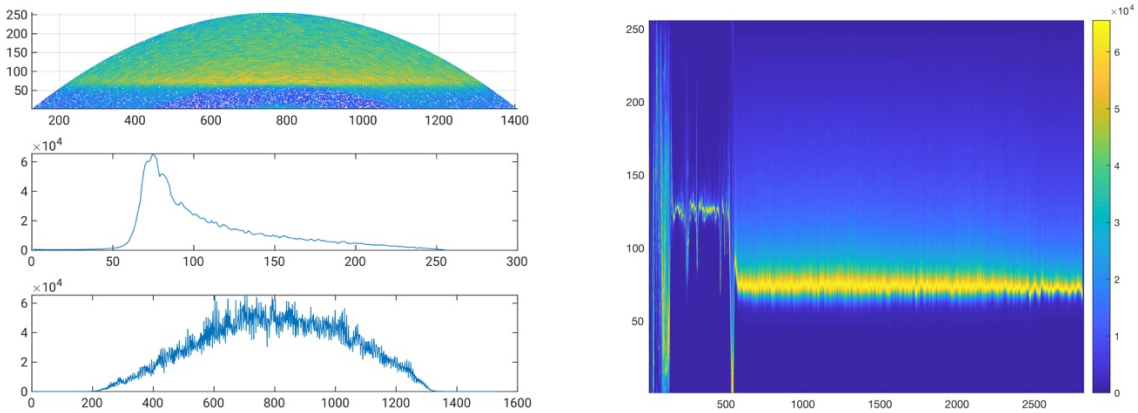

Fig.2 CS2 Stack, waveform and RIP LRMC-SAR for retracker SINCS_OV (left), waveforms (right)

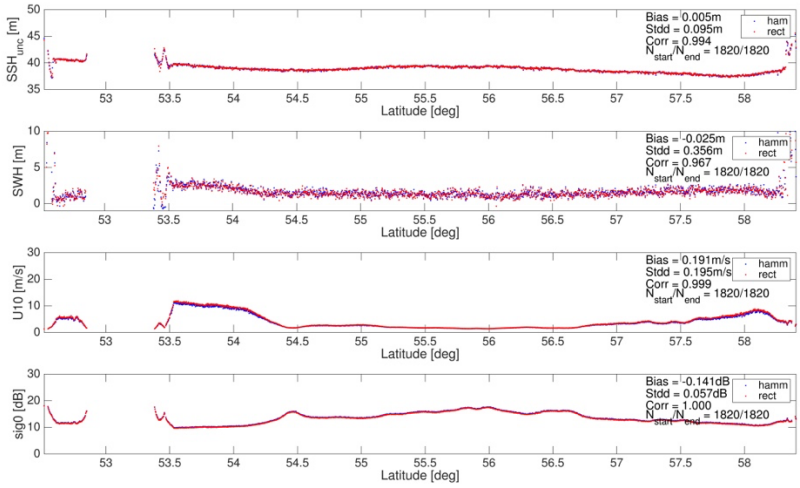


Fig.3 S3A. SINCS-OV_F1 with and without Hamming window, 1Hz.

Configuration files for Version 1.6 and Version 1.7 differ slightly, see Table 3 with differences in bold. The configuration file below is for Version 1.7 the for Task 1 (config_UF1_STD.txt)

```
#### FBR processor 1.7 config file
#### Flag to determine which offset for roll, pitch, time-tag and, reference-frame offset shall be used (CS2 only)
#### if 1, the same offsets as in RADS are used; If 0, the offsets used for CS2 Baseline C are used
USE_RADS_BIASES = 0

#### String to determine which implementation shall be used in L1/L2 processing, Options are C or Matlab
#### C:      C routines for the model based functions and for the  bottleneck in the L1B processing (C-Routines are much faster)
L1B.ProgLang = C
L2.ProgLang  = C

###Processing Flags: 0/1 (not used/used); RDS (Reduced SAR), SAR (unfocused SAR), RMC (Low Resolution Range Migration Corrected) or LRMC-SAR
L1B.Flag.RDS = 1
L1B.Flag.SAR = 1
L1B.Flag.RMC = 1

#### Number of burst considered in the focusing. If this value is set to one, no focusing will be applied. Options: 1, 4, 12, 20
L1B.Focus_Nb = 1

### Logical value determining if focused DDA processing shall be used even, if the number of bursts is one ( 0 := unfocused, 1 := focused )
L1B.Focus_DDA = 0

#### Cutoff Doppler frequency factor, which limits Doppler frequencies to: fD in [ DopplerCutoff * fDmin, DopplerCutoff * fDmax ]
L1B.DopplerCutoff = 0.75;

#### Retracker used to generate L2 for each processing scheme. These fields are ignored if the coresponding FLAG is zero
#### Choice for RdSAR: BMLE3, SINC2 and TALES Supported for others: SINCS and SINCS_OV, choice for all: NONE
#### Note 1: SINCS_OV is a stack retracker; 2: SINCS_OV works well only with none skewed distributed data, Note 3: NONE no retracking
L2.Retracker.RDS = SINC2
L2.Retracker.SAR = SINCS
L2.Retracker.RMC = SINCS

#### Pulse distribution (supported: 0:=Standard, 1:=Zero_Skewness )
L1B.Pulse_Skew = 0

#### Flag to determine if more realisitic antenna pattern shall be used
L2.Real_Antenna = 0

#### Number of reweighting iterations, which shall be performed, 0 (no reweighting), At this stage only SAR or LRMC-SAR is affected
L2.reweight = 0

#### Flag to determine if Stack shall be stored (much bigger output files). Stacks stored as 16 bit unsigned integer
NC.STK_Flag  =   0
NC.Echo_Flag =   0
NC.Chunk     = 480
```

### Zero padding flags: 1 means zero padding shall be applied, Only supported value at the moment is 1
**L1B.Zero_Padding_Range_Flag = 1**
**L1B.Zero_Padding_Along_Flag = 1**

#### L1B sampling frequency (supported: 20, 40, 80)
L1B.Sample_Freq = 20

#### Reference Surface used in the processing
###Sphere:  State of the art, local approximation as sphere see Chelton,
### Ellipsoid: Uses a reference ellipsoid locally
#### Slopes:  Sphericals Harmonics used to locally get surface slopes
#### Geoid:  Sphericals Harmonics used to locally approximate surface by torus
L1B.REF_SURF = **Geoid**

#### Along track window (supported: hamming and rect )
L1B.Win_Name = rect

#### Flag to determine which surface type is going to be retracked
#### Water -> All points identified as water are going to be retracked
#### Ocean -> Only Points with a distance to coast > 10 km will be retracked
#### All  -> Everything is going to be retracked
#### None  -> Nothing is going to be retracked
L2.RET_SURF = Ocean
L1B.input_folder = /Volumes/Elements/NEA/
NC.output_folder = /Users/cbuchhau/Desktop/EasternRun_Output/NEA_STD_UF1/

#### Time intervall which is going to be considered
#### Dateformat is: yyyy-mm-ddTHH:MM:SS
ROI.Time_Start = 2000-01-01T00:00:00
ROI.Time_End  = 2030-12-31T24:00:00

#### Area which is going to be processed to L1b (North South East and West border)
ROI.LAT_N =  70.0
ROI.LAT_S =  30.0
ROI.LON_E =  16.0
ROI.LON_W =  -15.0

#### Path and name of auxiliary files
#### Path to geoid file
AUX.GEOID_file = /Users/cbuchhau/Desktop/auxiliary/und_min1x1_eigen-6c4_Nmax2190_MeanTide_global.nc
AUX.DEV_file = /Users/cbuchhau/Desktop/auxiliary/dev_min1x1_eigen-6c4_Nmax2190_MeanTide_global.nc
#### Name of geoid model
AUX.GEOID_model = EIGEN-6C4

#### Path to mean sea level file
AUX.MSS_file = /Users/cbuchhau/Desktop/auxiliary/DTU15MSS_1min.nc
#### Name of MSL model
AUX.MSS_model = DTU15

#### Path to distance to coast grid file
AUX.DIST_file = /Users/cbuchhau/Desktop/auxiliary/dist_to_GSHHG_v2.3.7_1m.nc
#### Name of distane to coast grid
AUX.DIST_source = GSHHS v2.3.7 1m grid file

Table 4. Options in Vers 1.6 and Vers 1.7

| | TUDaBo 1.6 Linux | TUDaBo 1.7 Linux |
|---|---|---|
| USE ALWAYS 0 | USE_RADS_BIASES = 0 | USE_RADS_BIASES = 0 |
| MATLAB/C | L2.Matlab = 1 | L1B.ProgLang = Matlab<br>L2.ProgLang = Matlab |
| Processing | 1B.Flag.RDS = 1<br>L1B.Flag.SAR = 1<br>L1B.Flag.RMC = 1 | L1B.Flag.RDS = 1<br>L1B.Flag.SAR = 1<br>L1B.Flag.RMC = 1 |
| N. of burst | L1B.Focus = 1 | L1B.Focus_Nb = 1 |
| RETR | L2.Retracker.RDS = SINC2<br>L2.Retracker.SAR = SINCS<br>L2.Retracker.RMC = SINCS_OV | L2.Retracker.RDS = SINC2<br>L2.Retracker.SAR = SINCS<br>L2.Retracker.RMC = SINCS_OV |
| SKEWNESS | L1B.Pulse_Skew = 0 | L1B.Pulse_Skew = 1 |
| **Doppler Cutoff** | **NA** | **L1B.DopplerCutoff = 1** |
| RA only 1.7 | L2.Antenna_Flag = 0 | RA L2.Real_Antenna = 0 |
| **Reweighting** | **NA** | **L2.reweight = 0** |
| Stack<br>Waveform<br>Read burst | NC.STK_Flag = 0<br>NC.Dump_Echo_Flag = 0<br>NC.Chunk = 480 | NC.STK_Flag = 0<br>NC.Echo_Flag = 0<br>NC.Chunk = 480 |
| Only 1 allowed | L1B.Zero_Padding_Range_Flag = 1<br>L1B.Zero_Padding_Along_Flag = 1 | L1B.Zero_Padding_Range_Flag = 1<br>L1B.Zero_Padding_Along_Flag = 1 |
| (20, 40, 80) | L1B.Sample_Freq = 20 | L1B.Sample_Freq = 20 |
| T SINCS_OV_RMC | L1B.REF_SURF = Geoid | L1B.REF_SURF = Geoid |
| HAMMING | L1B.Win_Name_ts = rect<br>L1B.Win_Name_tf = rect | L1B.Win_Name = rect |
| | L2.RET_SURF = All | L2.RET_SURF = Ocean |

## 2.2 Sentinel-3

The TUDaBo processing for Sentinel-3 has been used and tested during the Hydrocoastal Project. With the "L1a to L1b" step an alternative L1b input data to the STARS retracker was prepared (Cotton et al, 2021, test data Internal note). Version 1.7 has both the standard DDA and the BPA option. The configs are the same as for CryoSat-2 (Table 2).

# 3 Validation

## 3.1 North Atlantic Region and input data

Results are produced in the German Bight and the Western Baltic Sea sub-region ($ROI_1$-NEA/GBWB Fig. 1) for time span 2010-2019. Conventional SAR processing was originally used in Version 1.6 (along-track FFT, Raney 1998) and compared with Back projection (available in version 1.7). Figure 4 gives the location of the Bfg tide gauge and the BSH buoys used in the in-situ validation of range, SWH and standard deviation of vertical velocities $\sigma_v$. This last is a the forth parameter output of the SINCS-OV retracker, in addition to the three standard, which are range, SWH and backscatter coefficient.

Figure 5 gived the time data coverage for each buoy. Black dot means that a CS2 point close enough in time (max. 20 minutes) and space (max. 20 km) was found.

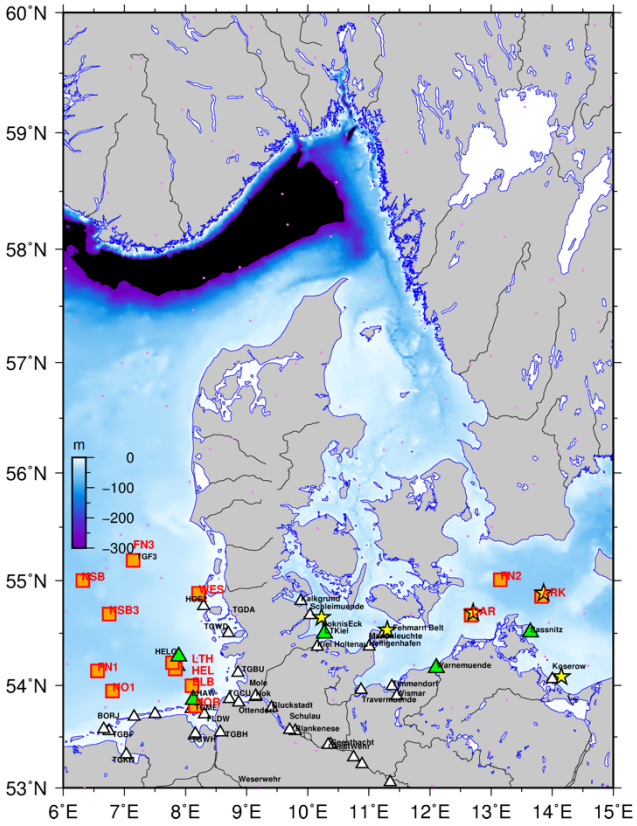


Fig.4 German Bight and Western Baltic ($ROI_1$-NEA/GBWB). Considered buoys (square orange) and tide gauge (green triangle). Not used tide gauge (white triangle) and permanent mooring (stars yellow)

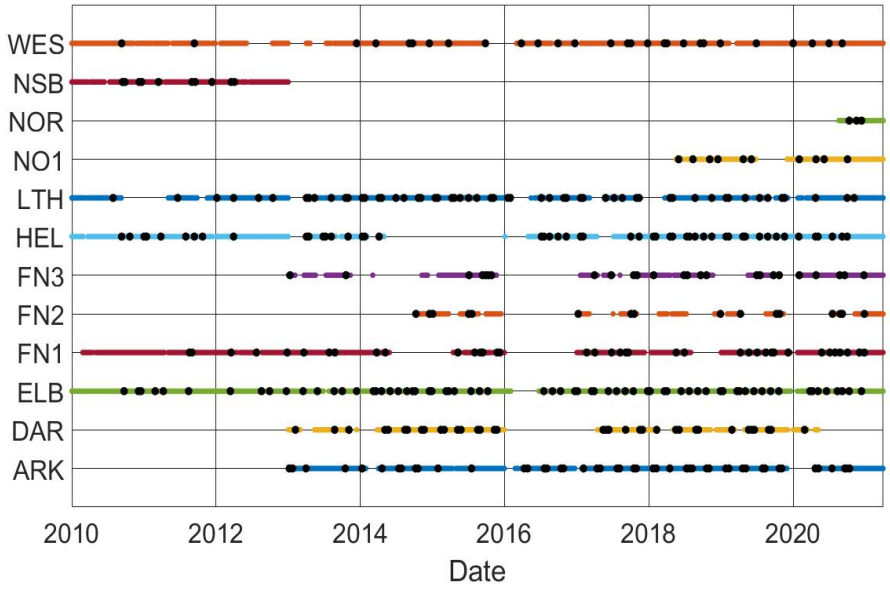


Fig.5 Buoys data coverage in German Bight and Western Baltic ($ROI_1$-NEA/GBWB), see Fig. 4 (from Buchhaupt et al., submitted).

## 3.2 Post-Processing

The uncorrected height SSH, obtained as orbit minus the uncorrected range output of each retracker, are corrected using the altimetric corrections available in the SAMOSA+ (Dinardo et al., 2017, 2019; Dinardo 2020) products given by *the EarthConsole®/Altimetry Virtual Lab* SARvatore services".

An altimeter time series is constructed using altimeter data located at least 5 km away from coast and between 5 and 10 km from the in-situ stations. For each track, we select the nearest 1 Hz altimeter point to the in-situ station. For SSH, a 3-sigma outlier criteria relative to the median is applied, which differs slightly from the criteria applied to SWH. The in-situ time-series are merged together in the two basins and the statistics of the merged data is computed for each basin.

For SWH the values larger than 1.5 times the interquartile range above the upper quartile or lower than the lower quartile are considered as outlier. This outlier test does not assume normal distributed data and therefore it is better suited for SWH and $\sigma v$ .

For SWH with the standard SAR DDA processing, the SWH SINCS-OV agrees at best with the buoys, as shown in Fig. 6. It has the lowest standard deviation of differences (STDD), the lowest mean difference and also the highest correlation. On the other hand, the SAR waveform retracker SINCS has the worst agreement, performing worst than the RDSAR results.
The agreement with the buoys is higher when using the ZSK distribution of pulses, compared to the use of the standard STD distribution. The same holds also when Backprojection Algorithm processing is applied, as shown in Fig. 7. The standard deviation, slope and bias are comparable.

Since only SINCS-OV is capable of estimating $\sigma_v$ no other retrackers can be compared with buoys. The agreement - presented in Fig. 8 is with a slope of 1.074, a correlation of 0.902, a STDD of 8.8 cm/s and a mean difference value of 0.8 cm/s.

A similar methodology as used for the buoys is applied in the validation of altimetric SSH against tide-gauges. Firstly, from the altimeter data we compute an "in-situ" height corresponding to the gauge readings as:

$$SLA_i = h_{unc} - h_{mss} - \Delta h_{iono} - \Delta h_{dry} - \Delta h_{wet} - \Delta h_{set} - 0.468\,\Delta h_{pole} - \Delta h_{load} + \mathrm{EMB} \quad (1)$$

with $h_{mss}$ mean sea surface from the DTU15 model, $\Delta h_{wet}$ wet tropospheric correction GDP1 solution of the GNSS-derived Path Delay Plus (GPD+) and the EMB derived in Buchhaupt et al. (submitted).
The sea state correction EMB $\Delta h_{ssb}$ does not include the tracking bias. As only SINCS-OV estimates the parameter $\sigma_v$ to retrieve the EMB correction, for SINCS and SINC2 $\sigma_v$ derived from the ERA5 $T_{02}$ parameter is used instead.
Ocean tide and dynamic atmospheric correction (DAC) corrections are applied to both altimetry and tide gauge data to obtain the sea level anomaly corrected for all the geophysical effects. The ocean tide is from the ocean tide TPXO9-ATLAS and the DAC correction from AVISO.

$$SLA = SLAi - \Delta h_{oct} - \Delta h_{DAC} \quad (2)$$

We demean altimeter and tide gauge time-series independently. Thus, the validation is relative and not absolute. We apply the 3-sigma outlier criteria relative to the median. Finally, only the common points are selected in the merged time-series. The comparison of the various retracking without applying the EMB correction is shown for the German Bight in Fig. 9 for the Standard Unfocused SAR and in Fig. 10 for the Back Projection Algorithm. All results give a similar precision and accuracy. The STDD is about 7 cm, the correlation coefficients are close to one and the regression slopes are around 0.97. All offsets are zero because the means of each series were removed. Of interest is the comparison with the EMB applied, shown in Figs. 9,10,11,12, right. Fewer points can be observed, which is caused by the data coverage of the wave model, used to calculate the EMB for SINCS and SINC2. For SINCS-OV, which considers the EMB with its $\sigma_v$ estimates, the STDD becomes 7 mm smaller and the slope gets closer to one, which leads to the assumption that the EMB improves the SLA accuracy. Similar conclusion can be drawn for SINCS and SINC2 results. Finally, similar conclusions are drawn for the stations merged in the Baltic Sea, see Figure 11, 12.

In addition to the in-situ validation we perform also validation of SWH using the ERA5 database. RDSAR is assumed to be not affected by the VMWP, therefore is used as reference solution for SINCS-OV ZSK (Buchhaupt, 2019). The mean differences between SAR SINCS-OV ZSK with respect to ERA5 SWH given in Fig. 13 (right) shows that agreement with respect to ERA5 SWH - compared to SAR SINCS (Fig. 13 middle) – improves significantly, which can be explained by the consideration of vertical wave particle velocities. The sea state dependent trend is very similar to those shown for SINC2 ZSK in Fig. 13 (left). Therefore, the SWH behaviour is very similar for SINCS-OV ZSK and SINC2 ZSK. This means that SWH estimates from RDSAR and SAR signals become more consistent. A paper, Buchhaupt et al., has been submitted to AdSR and included these and further results.

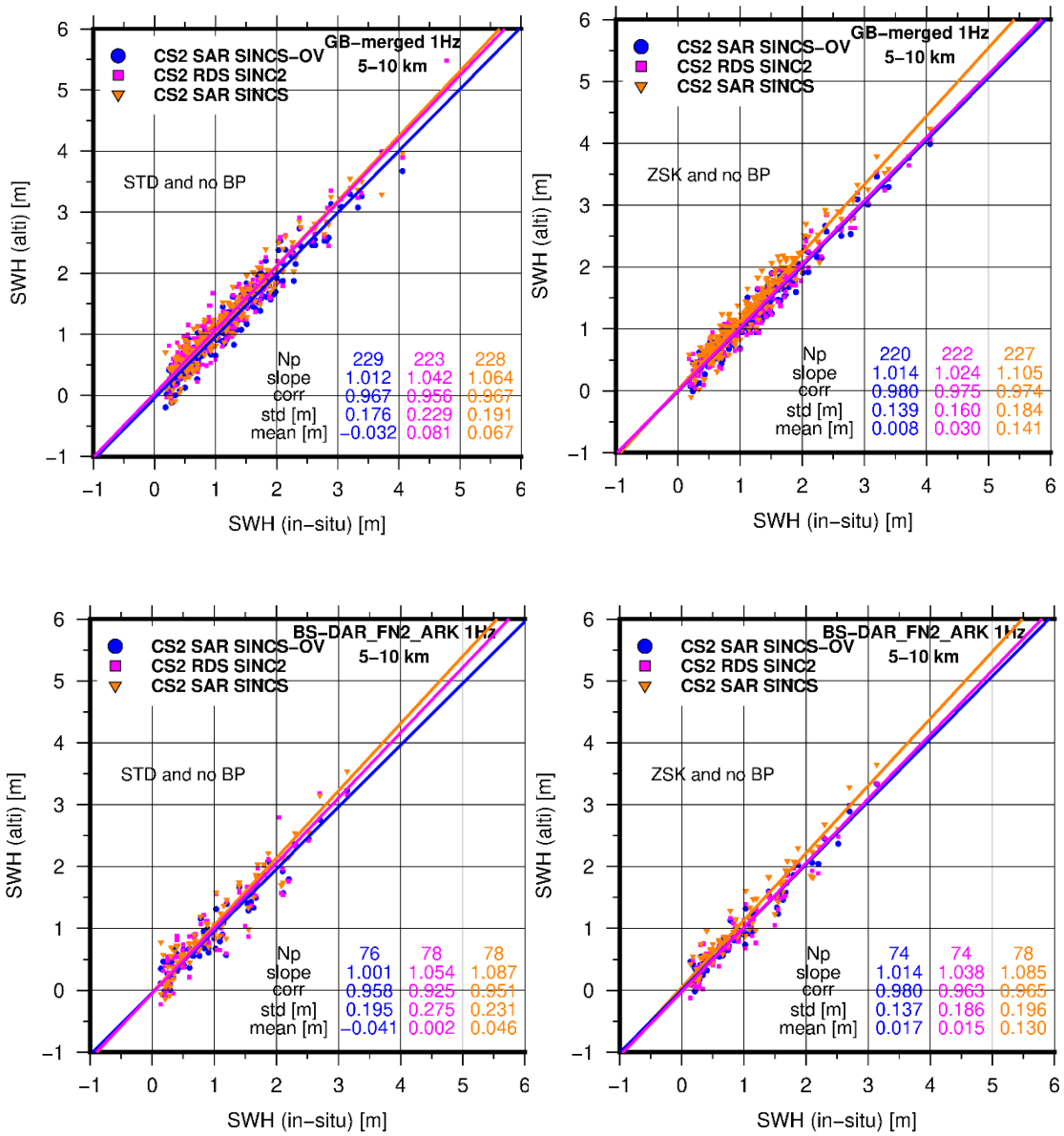


Fig. 6. CS2. Comparison of SWH between altimetry and merged buoys for the SINCS-OV, SAR and RDSAR L2 data (right) with distribution STD (left) and ZSK (right). Standard DDA processing in German Bight (above) and Baltic Sea (below). Results are at 1Hz.

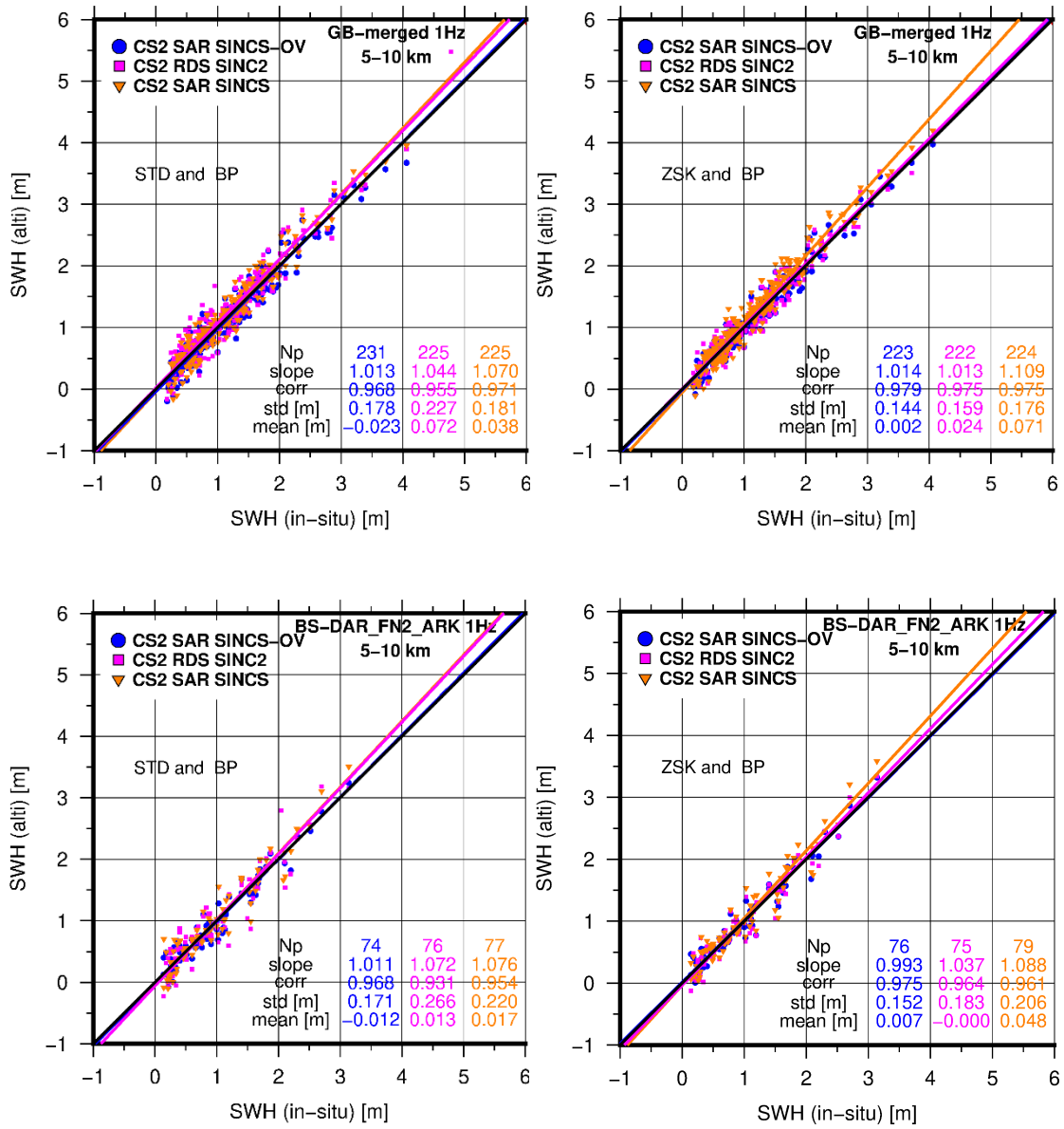


Fig. 7. CS2. Comparison of SWH between altimetry and merged buoys for the SINCS-OV, SAR and RDSAR L2 data (right) with distribution STD (left) and ZSK (right). SAR Backprojection processing in German Bight (above) and Baltic Sea (below). Results are at 1 Hz

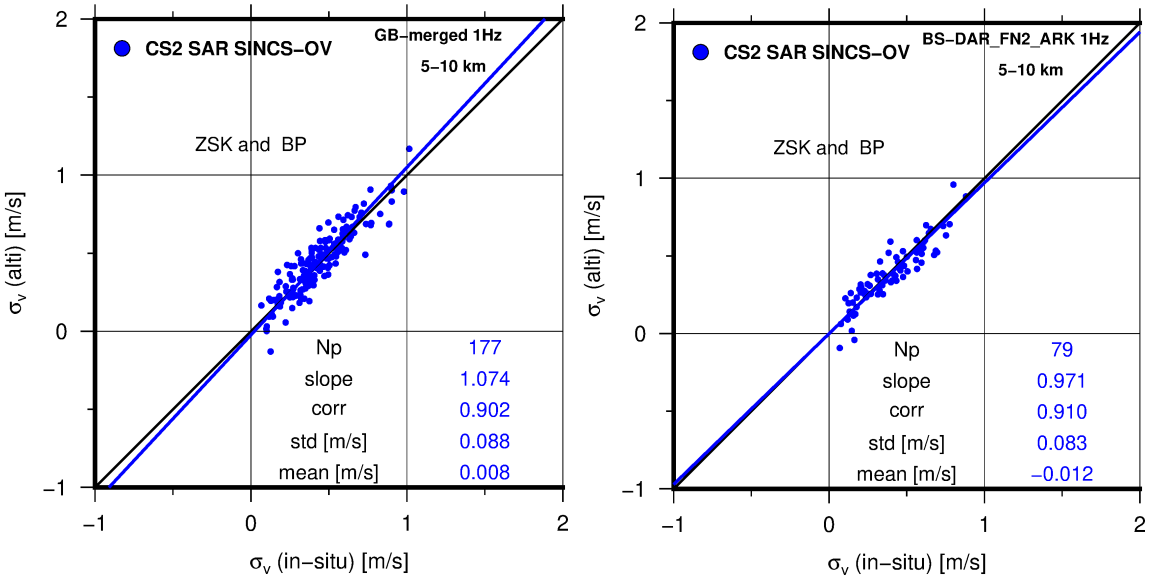


Fig. 8. CS2. Comparison of $\sigma v$ from SINCS-OV and from buoys located in the German Bight (left) and in Baltic Sea (right). Results are at 1 Hz.

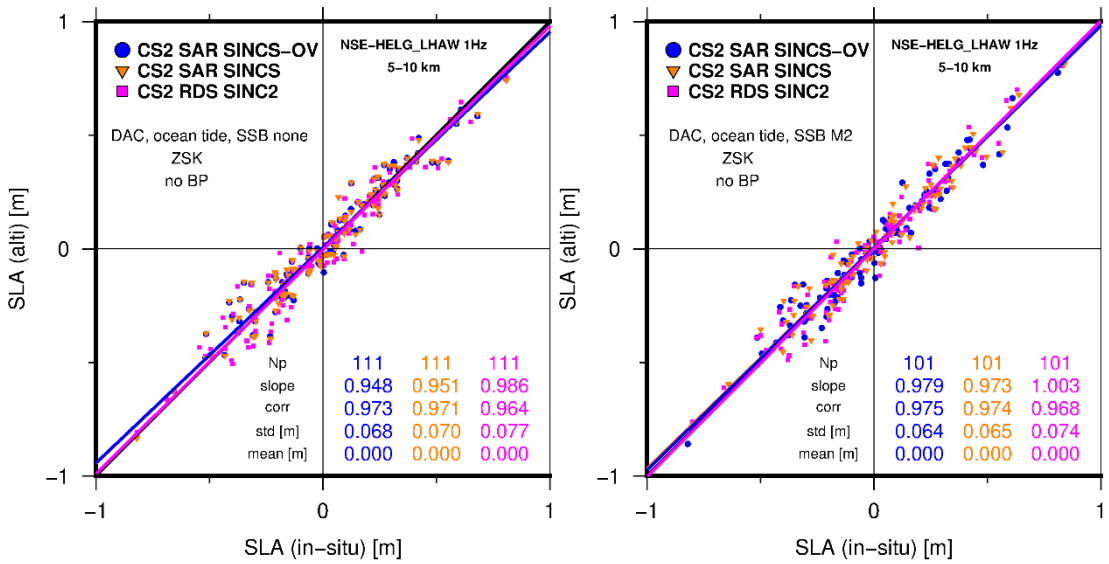


Fig. 9. CS2. Comparison of *SLA* from altimetry and from tide-gauges located in the German Bight. Altimeter is not corrected for an electromagnetic bias (left) and corrected (right). Standard unfocused SAR. Results are at 1Hz.

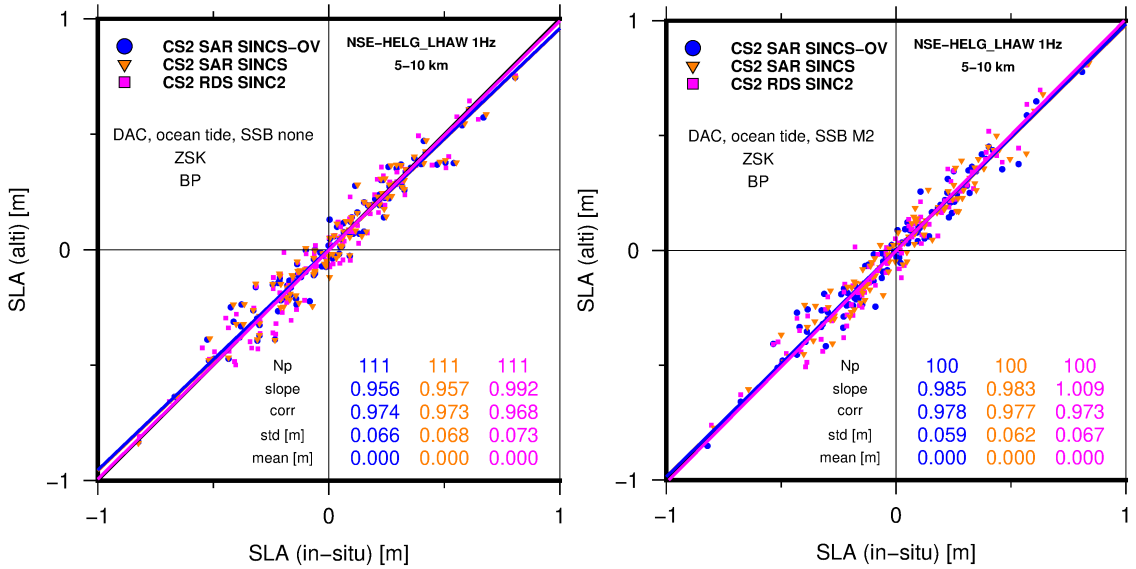


Fig. 10. CS2. Comparison of *SLA* from altimetry and from tide-gauges located in the German Bight. Altimeter is not corrected for an electromagnetic bias (left) and corrected (right). (from Buchhaupt et al., submitted). Back Projection Algorithm. Results are at 1Hz.

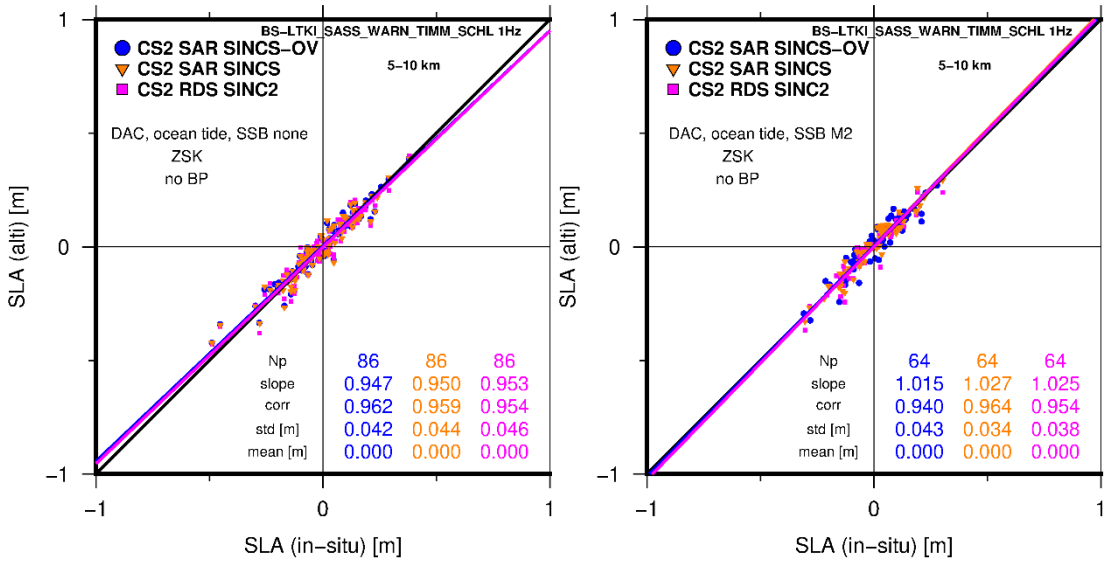


Fig. 11. CS2. Comparison of *SLA* from altimetry and from tide-gauges located in the Baltic Sea. Altimeter is not corrected for an electromagnetic bias (left) and corrected (right). Standard unfocused SAR. Results are at 1Hz.

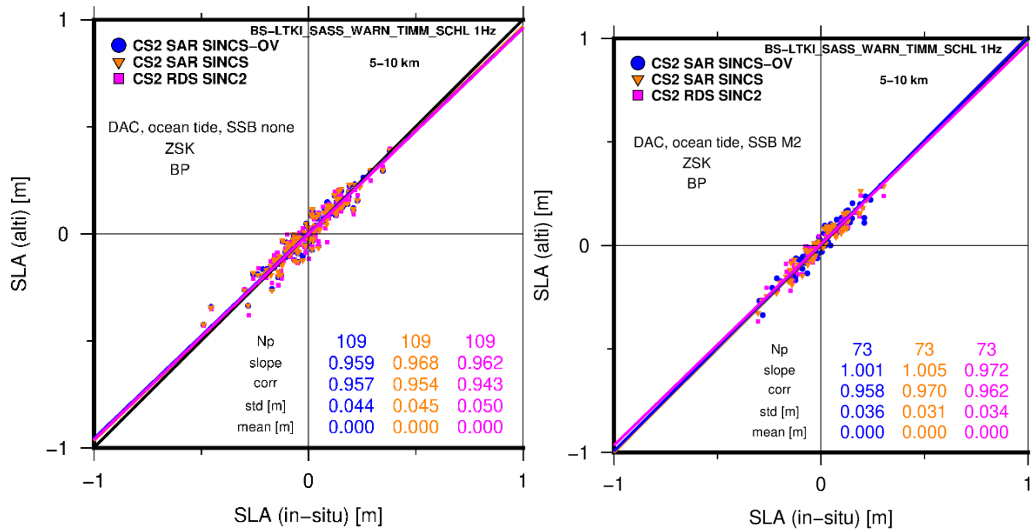


Fig. 12. CS2. Comparison of *SLA* from altimetry and from tide-gauges located in the Baltic Sea. Altimeter is not corrected for an electromagnetic bias (left) and is corrected for it (right). Back Projection Algorithm is used. Results are at 1Hz.

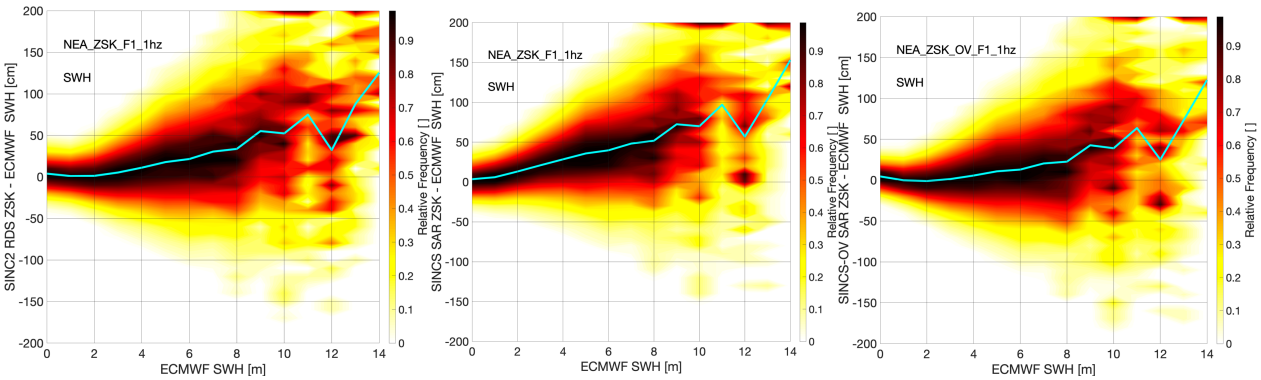


Fig. 13. CS2 in ROI1-NEA/GBWB sub-region. 2D histogram of differences between SINC2 RDSAR (left), SINCS SAR (middle) and SINCS-OV SAR (right) ZSK SWH and ERA5 SWH with respect to ERA5 SWH. The cyan colored line gives the mean differences with respect to ERA5 SWH. Results are at 1Hz (from Buchhaupt et al., submitted to AdSR).

Sentinel-3 data processed in TUDaBo are further used in master and bachelor thesis. Results for SINCS-OV processing for Sentinel-3 in year 2018 were presented at the Living Planet 2022. Fig. 14 shows the quartiles of absolute differences of consecutive 20-Hz Sentinel-3A data in ROI1-NEA/GBWB (presentation by C.Buchhaupt). The corresponding for CryoSat-2 is seen in Fig. 15. In both figures are shown also results for first attempt for the new retracker TALES-OV dedicated to coastal region. We suggest an extension of this CCN to further develop, validate and include also the TALES-OV retracker in our TUDaBo processing in Earth Console.

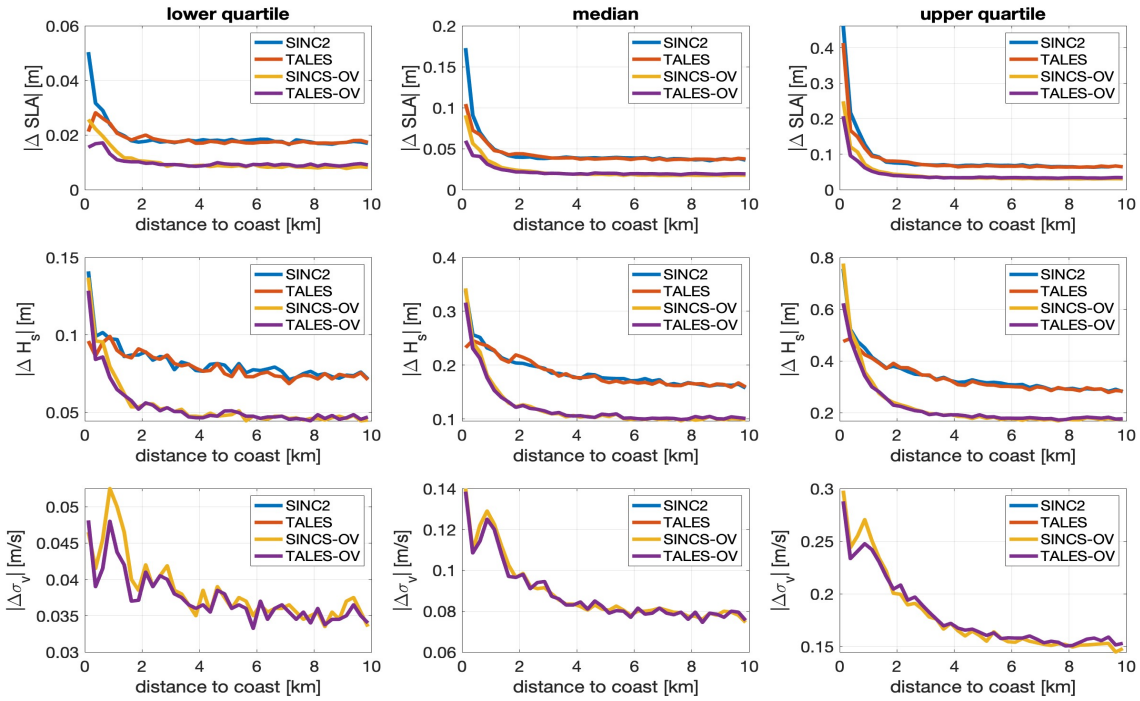


Fig. 14. Sentinel-3A quartiles of absolute differences of consecutive 20-Hz data in ($ROI_1$-NEA/GBWB (Living Planet 2022 presentation C.Buchhaupt et al.)

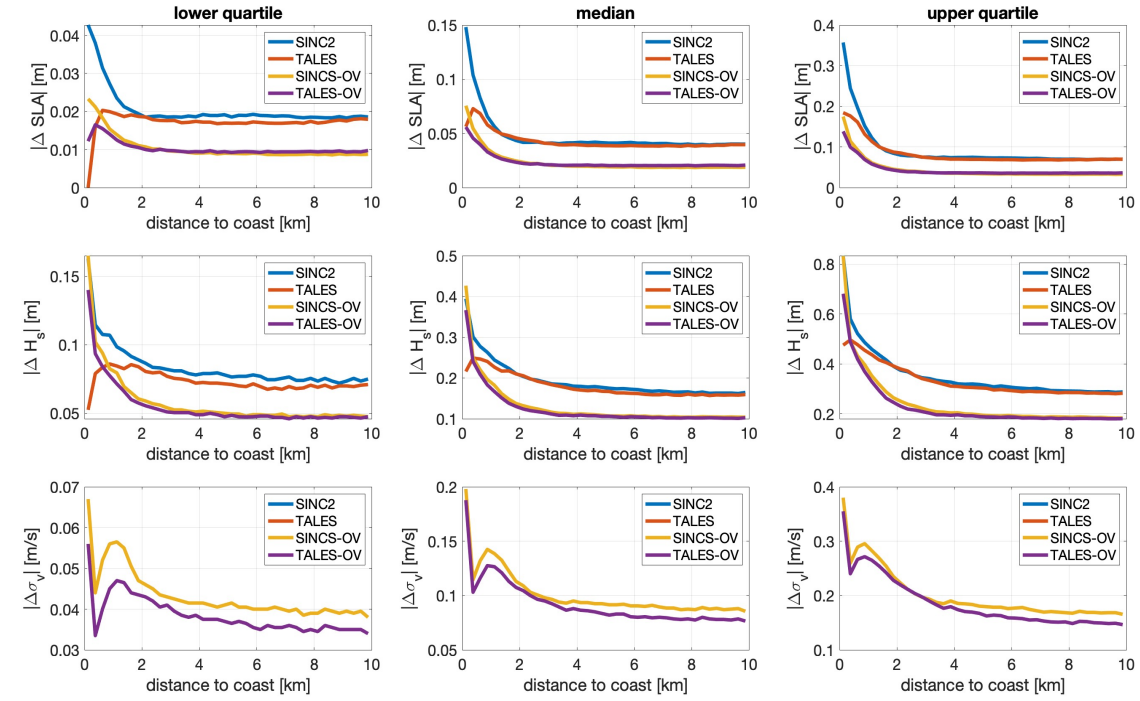


Fig. 15. CS2 quartiles of absolute differences of consecutive 20-Hz data in $ROI_1$-NEA/GBWB (Living Planet 2022 presentation C.Buchhaupt et al.)

## 3.3 Pacific Ocean with Marianna Trench

In regions with high geoid gradients the geophysical parameters may differ when computed using different surface for computation. We consider as second ROI a box in the Pacific Ocean including the Marianna Trench. We investigate here the difference in significant wave heights (SWH) and sea surface heights (SSH) obtained when using two different processing modes, for example SAR and LRMC. We make this comparison for the three reference surfaces: sphere, slopes and geoid (see processing options in Table 1). 1 year (2018) of Cryosat-2 data and 2 months (January and February 2019) of Sentinel-3 data are used. We see in Fig. 16 that SWH and SSH may differ by up to 0.7 m and 6 cm when using SAR and LRMC processing with the sphere as reference surface. Instead, when we use the geoid as reference surface almost no difference is found (Fig. 17). When we use the slope, the SSHs are different but not the SWH (Fig. 18). We conclude that the geoid should be used as reference surface when the LRMC processing is selected.

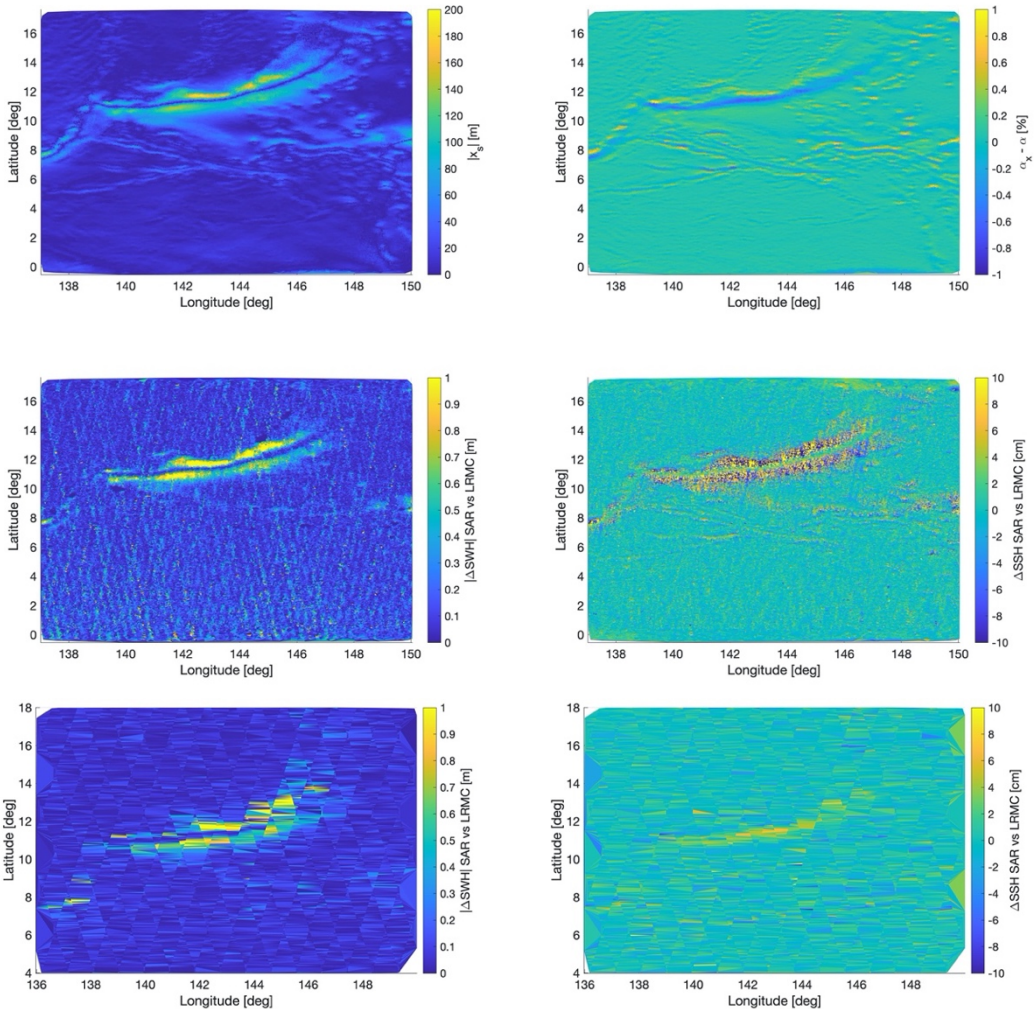


Fig. 16 Difference between SAR and LRMC results for SWH (left) and of SSH (right) for processing on the sphere. CryoSat-2 (middle) and Sentinel-3 (bottom). The top figures are the slope (left) and % difference in curvature between sphere and geoid.

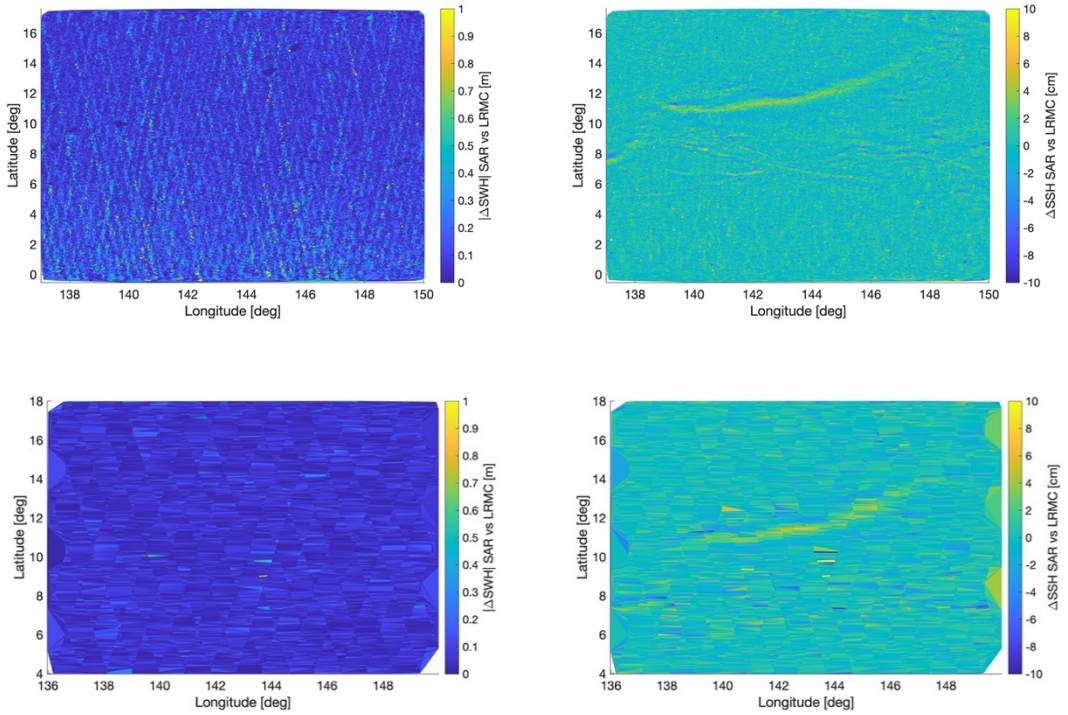


Fig. 17 SAR minus LRMC SWH (left) and of SSH (right) for "Slopes" reference surface. CryoSat-2 (top) and Sentinel-3 (bottom).

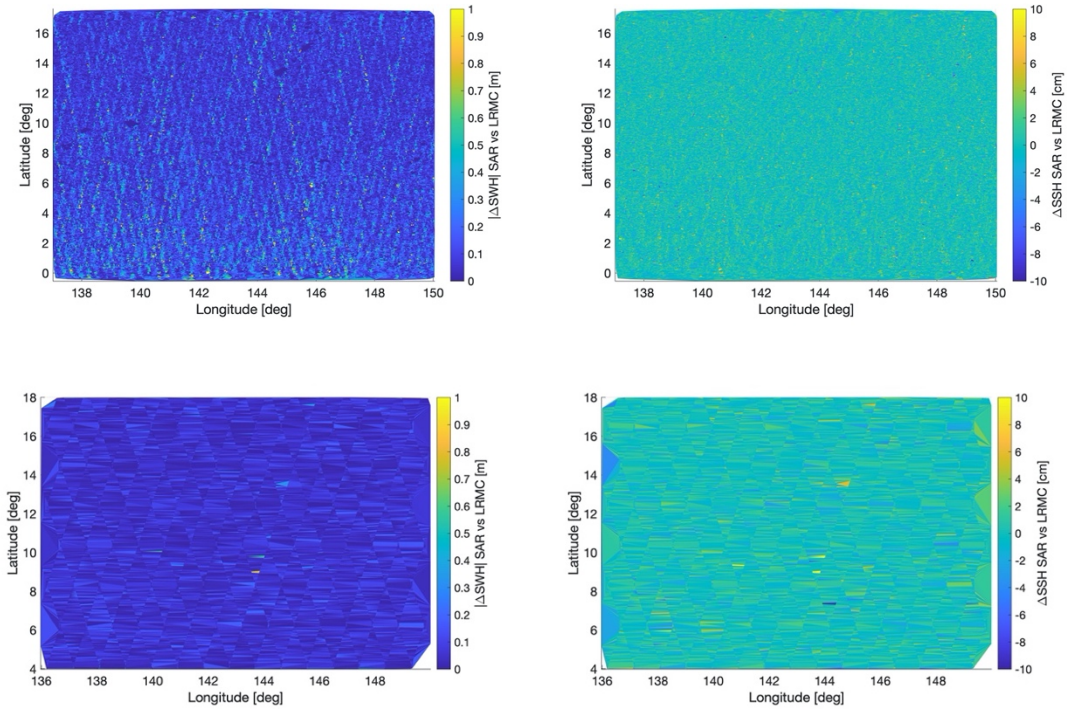


Fig. 18 SAR minus LRMC SWH (left) and of SSH (right) for "Geoid" reference surface. CryoSat-2 (top) and Sentinel-3 (bottom).

# 4 References

Buchhaupt C., Fenoglio-Marc L., Dinardo S., Scharroo R., Becker M (2017). A fast convolution based waveform model for conventional and unfocused SAR altimetry, Advanced Space Research Special Issue CryoSat-2, https://doi.org/10.1016/j.asr.2017.11.039

Buchhaupt C., Egido A., Smith W. H.F. and Fenoglio L. Conditional Sea Surface Statistics and Their Impact on Geophysical Sea Surface Parameters Retrieved from SAR Altimetry Signals, Adv. Space Research, https://doi.org/10.1016/j.asr.2022.12.034

Buchhaupt C., Egido A., Doug Vandemark, Smith W. H.F. and Fenoglio L. and Eric Leuliette (minor revision) Towards the Mitigation of Discrepancies in Sea Surface Parameters Estimated from Low- and High-Resolution Satellite Altimetry, Remote Sensing

Buchhaupt C. (2019). Model Improvement for SAR Altimetry. Ph.D. dissertation, Technische Universität, Darmstadt

Chelton, D. B.,Walsh, E. J., and MacArthur, J. L. (1989). Pulse compression and sea level tracking in satellite altimetry, Journal of Atmospheric and Oceanic Technology, 6:407–438.

Cotton D., A Garcia, M. Pattle, S Urien, L Fenoglio, Uebbing U., Stolzenberger S. (2021), *Test Data Set* - Technical Note, HYDROCOASTAL, SAR/SARin Radar Altimetry for Coastal Zone and Inland Water Level, Hydrocoastal

Dinardo, S., Fenoglio-Marc, L., Buchhaupt, C., Becker, M., Scharro, R., Fernandez, J., Benveniste, J., (2018). CryoSat-2 performance along the german coasts. Adv. Space Res. Spec. Issue CryoSat-2 62 (6), 1371–1404. https://doi.org/10.1016/j.asr.2017.12.018, ISSN 0273-1177.

Dinardo, S., Fenoglio-Marc, L., Buchhaupt, C., Becker, M., Scharro, R., Fernandes, J., Staneva, J., Grayek, S., Benveniste, J. (2020). A RIP based SAR Retracker and its application in North East Atlantic with Sentinel-3. Advances in Space Research, doi.org/10.1016/j.asr.2020.06.004.

Egido A. and W. H. F. Smith, "Fully Focused SAR Altimetry: Theory and Applications," IEEE Transactions on Geoscience and Remote Sensing, vol. 55, no. 1, pp. 392–406, Jan 2017.

Fenoglio-Marc, L., Dinardo, S., Scharroo, R., Roland, A., Dutour, M., Lucas, B., Becker, M., Benveniste, J., Weiss, R. (2015). The German Bight: a validation of CryoSat-2 altimeter data in SAR mode, Advances in Space Research, doi: http://dx.doi.org/10.1016/j.asr.2015.02.014

Fenoglio, L., Dinardo, S., Uebbing, B., Buchhaupt, C., Gärtner, M., Staneva, J., Becker, M., Klos, A., Kusche, J. (2021). Advances in NE-Atlantic coastal Sea Level Change Monitoring from Delay Doppler Altimetry, Adv. Space Res.,68(2), pp. 571–592, doi.org/10.1016/j.asr.2020.10.041.

Raney R.K. (1998). The delay/Doppler radar altimeter. IEEE Trans. Geoscience and Remote Sensing, vol. 36, pp. 1578–1588

# 5 List of acronyms

| | |
|---|---|
| ATBD | Algorithm Theoretical Baseline Documents |
| BPA | Back Projection Algorithm |
| CryoSat (-2) | ESA altimeter satellite for polar ice investigations |
| DDM | Delay Doppler Map |
| ESA | European Space Agency |
| F1 | Focused processing using 1 burst, uses the Back Projection Algorithm |
| L0 | Level zero (instrument telemetry) |
| L1A | Level 1A |
| L1B | Level 1B |
| L2 | Level 2 |
| LPF | Low-Pass Filter |
| LRM | Low Rate Mode |
| LRMC -SAR | Low resolution mode with applied range cell migration correction, in SAR mode |
| LRMC-F | LRMC focused, uses the BPA |
| NOAA | National Oceanic and Atmospheric Administration |
| PLRM | Pseudo Low Resolution Mode |
| RDSAR | Reduced resolution SAR mode data (used to generate PLRM) |
| RIP | Range Integrated Power |
| SAR | Synthetic Aperture Radar |
| Sigma0 | Radar Backscatter at nadir |
| SINC2 | SINCS based RDSAR retracker |
| SINCS | SINCS based SAR retracker |
| SINCS-OV | SINCS including vertical wave orbital velocities |
| SSH | Sea Surface Height |
| SWH | Significant Wave Height |
| TUDaBo | TU Darmstadt and University of Bonn |
| UF1 | Unfocused processing using 1 burst, uses the standard SAR processing |

# List of Acronyms References

Buchhaupt C., Fenoglio-Marc L., Dinardo S., Scharroo R., Becker M (2017). A fast convolution based waveform model for conventional and unfocused SAR altimetry, Advanced Space Research Special Issue CryoSat-2, https://doi.org/10.1016/j.asr.2017.11.039

Buchhaupt C., Egido A., Smith W. H.F. and Fenoglio L. (submitted). Conditional Sea Surface Statistics and Their Impact on Geophysical Sea Surface Parameters Retrieved From SAR Altimetry Signals, submitted to IEEE TRANSACTIONS ON GEOSCIENCE AND REMOTE SENSING

Buchhaupt C. (2019). Model Improvement for SAR Altimetry. Ph.D. dissertation, Technische Universität, Darmstadt

Chelton, D. B.,Walsh, E. J., and MacArthur, J. L. (1989). Pulse compression and sea level tracking in satellite altimetry, Journal of Atmospheric and Oceanic Technology, 6:407–438.

Cotton D., A Garcia, M. Pattle, S Urien, L Fenoglio, Uebbing U., Stolzenberger S. (2021), *Test Data Set* - Technical Note, HYDROCOASTAL, SAR/SARin Radar Altimetry for Coastal Zone and Inland Water Level, Hydrocoastal

Dinardo, S., Fenoglio-Marc, L., Buchhaupt, C., Becker, M., Scharro, R., Fernandez, J., Benveniste, J., (2018). CryoSat-2 performance along the german coasts. Adv. Space Res. Spec. Issue CryoSat-2 62 (6), 1371–1404. https://doi.org/10.1016/j.asr.2017.12.018, ISSN 0273-1177.

Dinardo, S., Fenoglio-Marc, L., Buchhaupt, C., Becker, M., Scharro, R., Fernandes, J., Staneva, J., Grayek, S., Benveniste, J. (2020). A RIP based SAR Retracker and its application in North East Atlantic with Sentinel-3. Advances in Space Research, doi.org/10.1016/j.asr.2020.06.004.

Egido A. and W. H. F. Smith, "Fully Focused SAR Altimetry: Theory and Applications," IEEE Transactions on Geoscience and Remote Sensing, vol. 55, no. 1, pp. 392–406, Jan 2017.

Fenoglio-Marc, L., Dinardo, S., Scharroo, R., Roland, A., Dutour, M., Lucas, B., Becker, M., Benveniste, J., Weiss, R. (2015). The German Bight: a validation of CryoSat-2 altimeter data in SAR mode, Advances in Space Research, doi: http://dx.doi.org/10.1016/j.asr.2015.02.014

Fenoglio, L., Dinardo, S., Uebbing, B., Buchhaupt, C., Gärtner, M., Staneva, J., Becker, M., Klos, A., Kusche, J. (2021). Advances in NE-Atlantic coastal Sea Level Change Monitoring from Delay Doppler Altimetry, Adv. Space Res.,68(2), pp. 571–592, doi.org/10.1016/j.asr.2020.10.041.

Raney R.K. (1998). The delay/Doppler radar altimeter. IEEE Trans. Geoscience and Remote Sensing, vol. 36, pp. 1578–1588